

Article

Significance of Features from Biomedical Signals in Heart Health Monitoring

Mohammad Mahbubur Rahman Khan Mamun 

Department of Electrical and Computer Engineering, Tennessee Technological University,
Cookeville, TN 38505, USA; mrkhanmamun42@tntech.edu

Abstract: Cardiovascular diseases require extensive diagnostic tests and frequent physician visits. With the advance in signal processing and sensor technology, now it is possible to acquire vital signs from the human body and process the signal to extract features necessary to primarily diagnose symptoms of cardiovascular disease early. This can help prevent deadly health incidents such as heart attack and or stroke, as well as reduce the number of visits to a health care facility. The proper detection of an elevated ST segment of ECG wave at an early stage may save the patient from having a heart attack or ST elevated myocardial infarction later. The use of a variety of complementary biomedical sensors can lead to a better diagnosis than what is possible when a single sensor is used. This paper proposes a MATLAB GUI which can detect elevated ST segments of ECG waves and use information from a variety of biomedical sensors to bring forth a technique to assess heart health to predict potential heart failure conditions. The proposed technique used fusion among multiple biomedical sensors to reduce the false alarm in diagnosis. Data from the online dataset were used to show the effectiveness and promise of the proposed detection of elevated ST segments and diagnosis techniques using the GUI.

Keywords: ST-segment detection; myocardial infarction; MATLAB; ECG; biomedical signal analysis



Citation: Mamun, M.M.R.K. Significance of Features from Biomedical Signals in Heart Health Monitoring. *BioMed* **2022**, *2*, 391–408. <https://doi.org/10.3390/biomed2040031>

Academic Editors: U Rajendra Acharya and Oliver Faust

Received: 20 October 2022
Accepted: 2 November 2022
Published: 10 November 2022

Publisher's Note: MDPI stays neutral with regard to jurisdictional claims in published maps and institutional affiliations.



Copyright: © 2022 by the author. Licensee MDPI, Basel, Switzerland. This article is an open access article distributed under the terms and conditions of the Creative Commons Attribution (CC BY) license (<https://creativecommons.org/licenses/by/4.0/>).

1. Introduction

Use of real-time biomedical signal analysis can be used to detect symptoms of risky heart diseases. This would allow patients to get proper and early treatment. Though the blood pressure and oxygen saturation give a discrete value, the ECG signal varies from individual to individual in terms of the waveform. This paper discusses how to use general real-time data to predict heart conditions. Based on the decision algorithm, the person will be advised to take the necessary measures. Myocardial infarction occurs when a lack of oxygen in heart tissue causes eventual death of that tissue if the supply does not get restored within a short time [1]. In reference [2], a combination of ECG signal and arterial blood pressure was used to classify heart disease, but during diagnosis, only heart rate was used as a feature. Although that was effective for arrhythmia detection, it was not sufficient for advanced heart issues. In [3], the work involved the use of blood pressure, ECG, respiration, and movement data, but was limited to the collection and storage of biomedical data. The work of [4], where biomedical data were collected and sent to a remote server, has similar limitations to that of [3]. Furthermore, the use of stand-alone devices is cumbersome and expensive. A hardware solution that integrates all the sensors used by the stand-alone devices will be more advantageous.

Recent developments in machine learning also allow the researcher to apply those for the diagnosis of many types of diseases [5–10]. For example: analyzing the ECG signal brings forth useful features, which can be used as input for machine learning algorithms to classify heart diseases. The problem is that the ECG data and other biomedical data are highly unbalanced, and they cause more challenges for typical machine learning algorithms. Many researchers proposed different techniques involving using biomedical data and

machine learning algorithms for heart disease diagnosis. Other than the imbalanced dataset, another limitation of using ML algorithms is the lack of proper explanation of the model's characteristics or behavior while making diagnostic predictions [11,12]. Additionally, due to imbalanced data, the business for the class with major data support constitutes another constraint [13–16].

A study proposed a technique where information from blood pressure and one ECG lead combined to detect (premature) ventricular contraction [17]. The limitation of their design is they have not considered any other lead information and haven't included central venous pressure (the blood pressure in the venae cavae near the right atrium). In 2007, the first implanted biotelemetry system for simultaneous measurement of blood flow, pressure, ECG, and the temperature was designed and implemented on animals by Axelsson et al., which had a bidirectional radio-frequency link that allowed the implant to send data as well as receive a command to implement [18]. They have performed testing on small animals and successfully communicated with the implanted machine for storage and implementation commands. Based on the result from the correlation analysis of abnormal ECG signal, extraction of parameters from the lobe and shape of the correlation function is easier through normalized autocorrelation and cross-correlation [19]. The same pattern was observed during normal ECG, and variation of the pattern was found for ventricular tachyarrhythmia and arrhythmias. Lovell et al. proposed a design of self-administered functional health status indices using remote monitoring of parameters of vital signs such as ECG, blood pressure, respiratory symptoms, movement, etc. [20]. Valerie et al. proposed a device that combines the signal from different sensors (which procures vital signs), which are Bluetooth enabled or integrated into the smartphone. After that, the smartphone processes the sensor data and monitors the patient's well-being and, in case of emergency calls, provides a message to a caregiver or a concerned person [21]. Considering heart monitoring, their proposal is limited to heart rate only using one lead, which restricts its ability to encounter complex heart diseases such as heart attack or block.

MI can occur without any major symptoms, so early detection is very crucial [22]. Deep learning techniques, such as convolutional neural networks (CNN) have been used to classify atrial and ventricular fibrillation as well as ST-segment elevation [23]. The main limitations are large amounts of data are required to train the algorithms, and CNN itself requires extensive computational resources. Using FPGA, Tang X et al. prepared a model to classify different features from ECG such as QRS complex and Q and T wave with high accuracy [24]. The AutoML technique has been used to obtain an optimal pipeline to classify ST segment-based abnormality [25,26]. Numerous studies have investigated ECG signals to detect heart disease using artificial intelligence (deep learning) [27–33] but, in general, the main drawbacks are the use of a very complex framework to build predictive models, hard-to-develop hardware from those models, and the imbalance of data among different classes [34].

Until now, a significant amount of research has been conducted for different kinds of arrhythmia detection which require features from the rhythm of the heart only, but diseases such as myocardial infarction require a complex relationship between the features from different sensors to diagnose the symptoms. In this paper, a technique for ST segment from ECG and symptoms for MI has been proposed using a biomedical signal processing technique. Additionally, fusion among several biomedical signals was implemented to diagnose symptoms for MI. A MATLAB GUI is presented where the whole feature detection and diagnosis prediction was implemented.

2. Background Information

The following sections will cover the necessary background information required for the experiment.

2.1. Functioning of Heart

The heart is the most crucial organ in the cardiovascular system, and it is responsible for supplying the blood with oxygen and nutrients. The heart is made up of four chambers: the right Atrium (RA), the left Atrium (LA), the right ventricle (RV), and the left ventricle (LV), as shown in Figure 1.

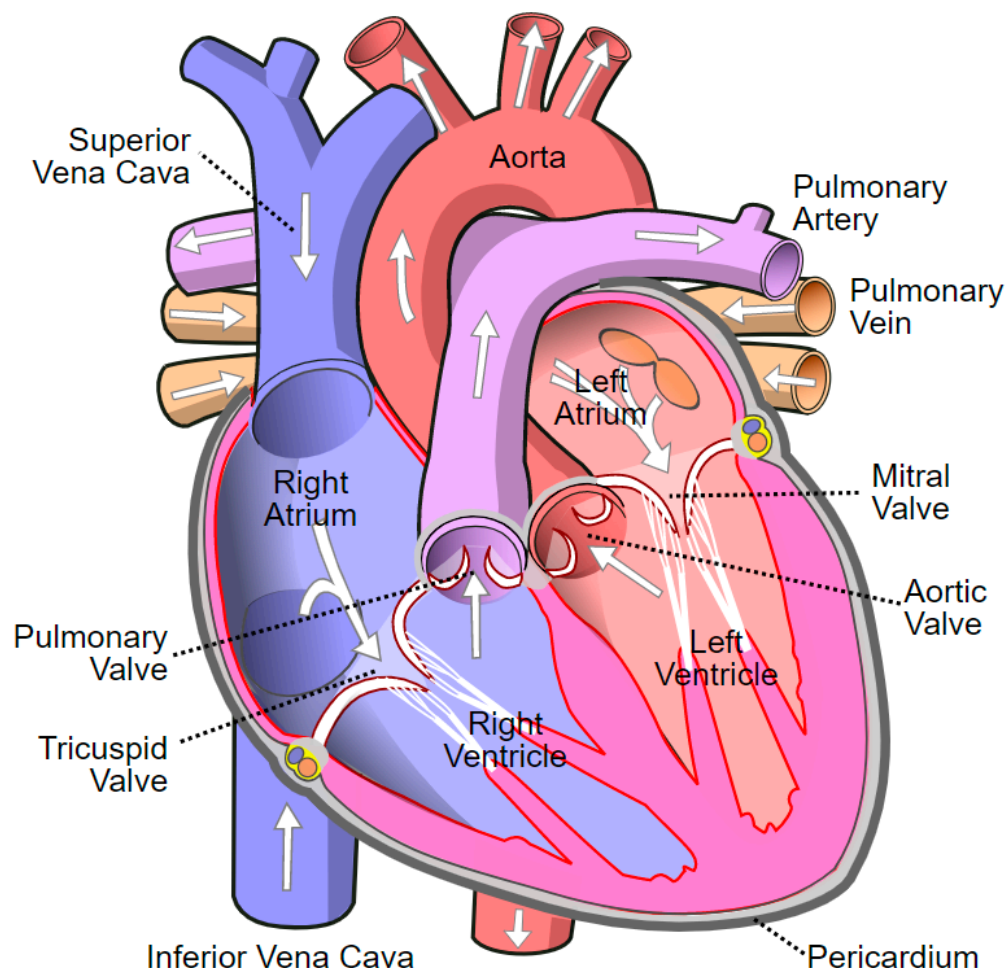


Figure 1. Anatomy of the human heart [35] © CC0 License.

Acute coronary syndrome (ACS) contributes to a significant share of mortality among all coronary heart diseases (CHDs). Among those, the ST segment elevation-related myocardial infarction (STEMI) is responsible for 30% of all ACSs [36,37]. There are still challenges to coming up with a timely diagnosis of STEMI. During myocardial infarction, there are changes in cardiac biomarkers (for example, ECG changes, evidence in other biomarkers, and changes in the image of loss of viable myocardium) [38]. When the ST segment in two contiguous ECG leads is greater than 2 mm for men, and greater than 1.5 mm for women with lead V2 and V3, it officially can be addressed as myocardial infarction.

2.2. ECG Leads

The most common arrangement for ECG testing is 12 leads. Among those, three leads are located on limbs, which are lead I, lead II, and lead III, as shown in Figure 2. These three leads constitute a lead system called Einthoven's triangle [3].

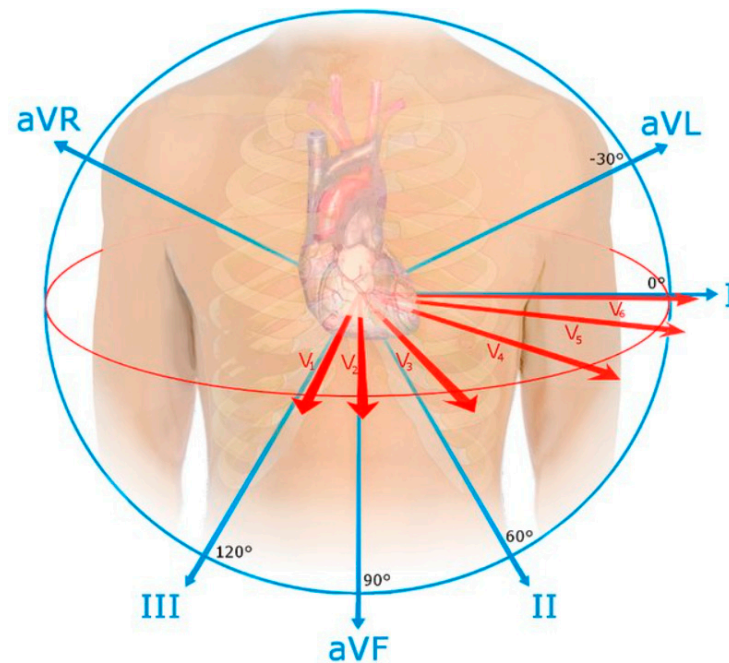


Figure 2. The standard 12-Lead ECG placement [39] © CC BY SA 4.0.

P wave shows the amplitude level of voltage signal (low), representing depolarization and contraction of the right and left atria [4]. Sinus rhythm is a clear P wave before the onset of the QRS complex. Ventricular rhythm or atrial fibrillation may cause the absence of a P wave. The QRS complex is the highest voltage deflection in a cardiac cycle; its magnitude depends upon age, gender, and body size. Ventricular depolarization happens during the time of the QRS complex, so any block or thickening of ventricular muscle will be indicated by a different QRS complex than usual [5]. T wave shows ventricular repolarization, and a large T wave may represent ischemia or hyperglycemia [6]. In Figure 3, the peak information of the ECG wave has been depicted.

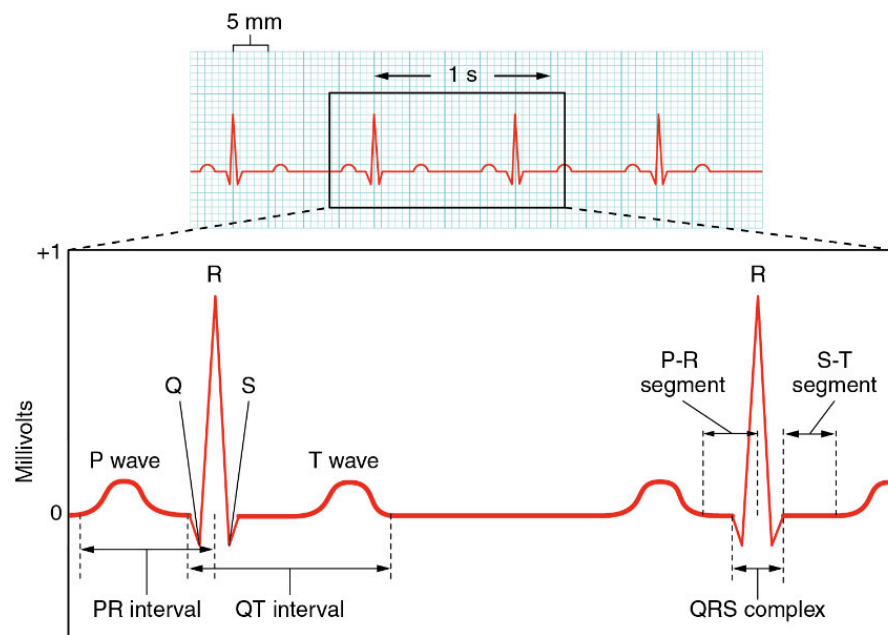


Figure 3. A sample of a normal ECG signal of a healthy subject [40]. © CC BY SA 4.0.

When blood supply gets slowed down or disrupted to a particular area of the heart, as shown in Figure 4, first ischemia occurs, then necrosis occurs, and eventually scarring of tissue occurs [41].

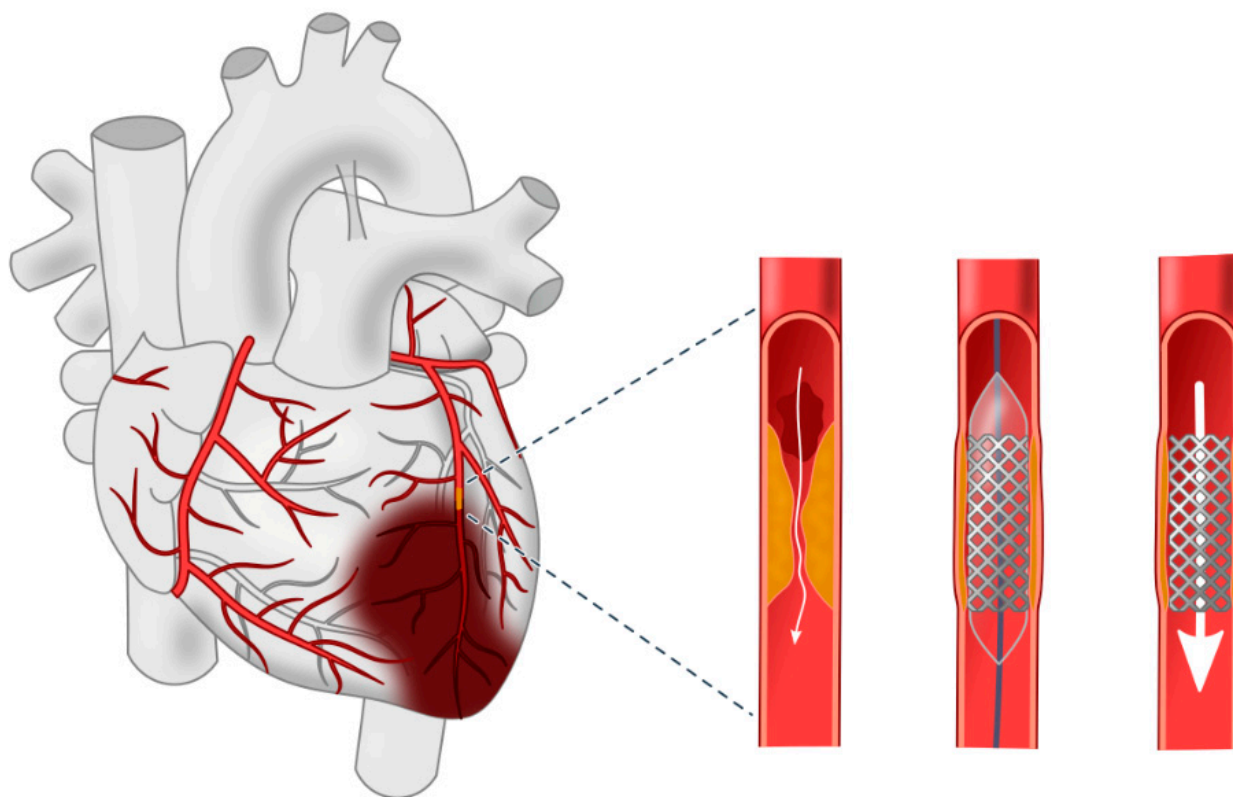


Figure 4. Myocardial Infarction area [42] © CC BY SA 4.0.

3. Materials and Methods

At the start of the process where the goal is to reduce the false alarm probability while detecting MI, the raw measurements from a variety of sensors are processed to remove unwanted noises. Then, algorithms for required feature extraction are implemented. The sensor data fusion is performed and correlated with MI symptoms to get appropriate heart condition decisions. This proposed idea brings techniques of biomedical signal processing, sensor data fusion, as well as decision algorithms together, to help people get diagnostic information about a heart condition. A conceptual diagram has been depicted in Figure 5, indicating data acquisition, pre- and post-processing of the data, feature extraction, and the fusion of features for decision. Cardiovascular system parameters which are used for the regulation of hemodynamic nature are strongly correlated [43]. Figure 6 shows a correlation between the RR interval and the pulse pressure interval. In the X axis, the R-R interval has been used. The R-R interval comes from the calculation from the distance between two R peak distances (consecutive). The Y axis contains a PP interval, which comes from the distance between consecutive pulse pressure wave peaks. The figure depicts the fact that the change in the RR interval and the PP interval increases proportionally. Additionally, it has been proven that pulse pressure amplitude is a marker of myocardial infarction risk, and the mean systolic blood pressure is significantly higher in MI participants [43].

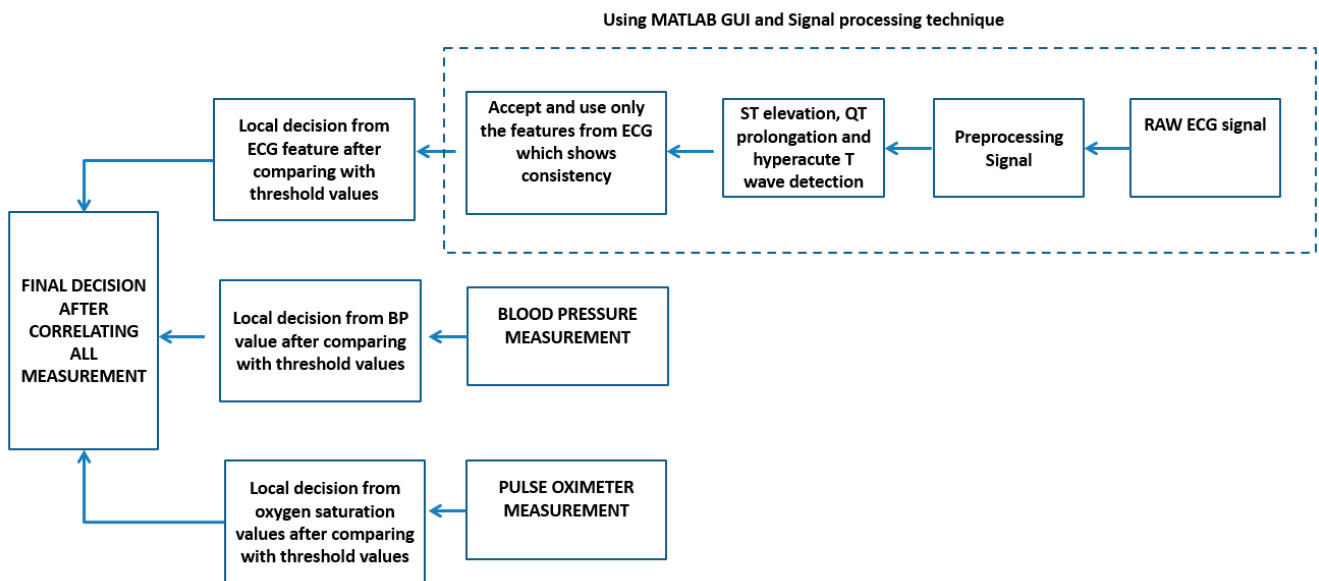


Figure 5. Proposed block diagram of ECG processing and sensor data fusion.

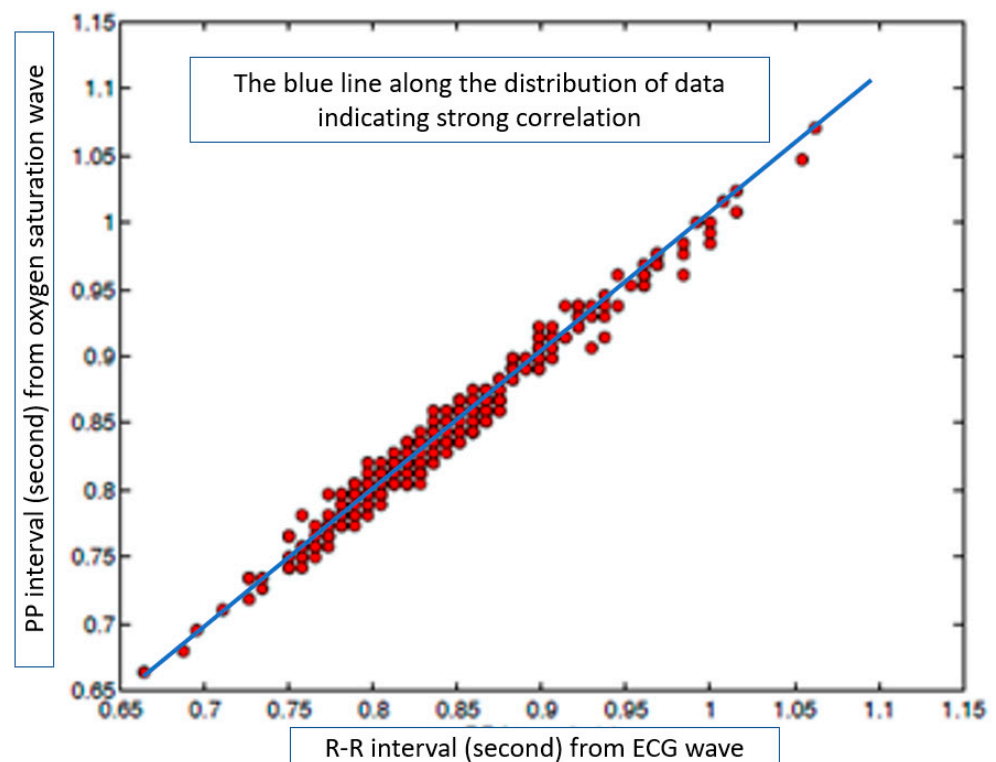


Figure 6. Correlation between a R–R peak interval from the ECG wave and the peak-to-peak interval from the oxygen saturation wave [44].

So, if an ECG alarm is triggered, the arterial blood pressure waveform will be checked for features extracted that either corroborate with the condition of ECG which triggered the alarm or not. Another way of viewing it is that the PPG waveform possesses different noise characteristics than blood pressure or ECG wave due to measurement technique and location. So, in some situations, the PPG waveform might provide more information than ABP or ECG in terms of heart rate variability.

3.1. Dataset and Preprocessing

The MIMIC database [45] was used for ECG, pulse oximeter, and blood pressure data of healthy and diagnosed MI patients. Each recording lasted for 10 s, with an average cycle number of 10. The range for systolic and diastolic blood pressure is 60 mmHg to 150 mmHg. While recording, the ECG 12-bit resolution was used, and the sampling rate was 500 samples/second. The ECG signal is naturally noisy, including electromagnetic interference, power line interference, muscle movement, baseline wander, etc. The signal was normalized by removing the baseline wander. Then, the FIR band pass filter and median filter were used to denoise the signal. To preserve the time and frequency content of the signal frequencies, wavelet transform [46] is used. The rationale behind choosing the ST segment is that research has shown that emphasizing the ST segment increases the chance of diagnosis using MRI up to between 50% and 84% [46]. Additionally, the rationale behind using the Q wave is that it is proven in research that prior or current MI creates a pathological Q wave, QT prolongation, or a hyperacute T wave [46]. A MATLAB GUI, as shown in Figure 7, was developed, which goes through each ECG wave and extracts necessary features which can be used later for the detection of symptoms of MI.

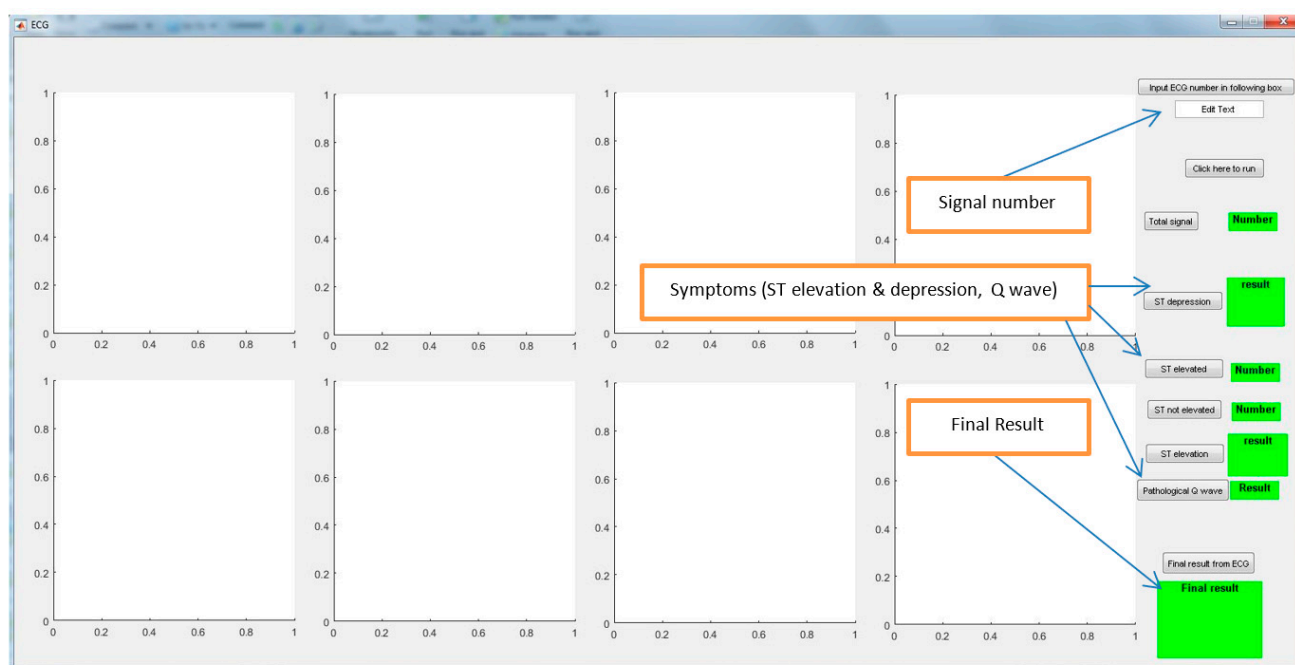


Figure 7. A MATLAB GUI to extract features from biomedical signals.

The most common choice for researchers for the analysis of ECG signals is the biorthogonal wavelet [47]. This wavelet can conserve time-dependent information on the ECG wave. So, it can be used to calculate the QRS peak with high accuracy along with other significant peaks from ECG waves. The scale and transition of wavelet transform keep the frequency, as well as time domain information, intact if the choice of mother wavelet is optimum. The bi-orthogonal wavelet has shown a high correlation with ECG waves, proving the significance of its use here. To make an appropriate choice of basis function for the wavelet, the desirable properties for ECG parameter extraction are symmetric, so that the maximum can be detected as maxima; also, a minimum number of sign changes is desirable to simplify the parameter extraction process. Using the chosen wavelet, the decomposition of the ECG wave was conducted in four scales (2^1 to 2^4). The interference and noise are found in the first two levels (2^1 – 2^2), and most of the energy of the QRS complex of each ECG wave was found in the last two levels (2^3 – 2^4).

3.2. Decision from the Sensor

The national early warning score (NEWS) is an indexing system used to determine the degree of illness of a patient during critical care intervention. NEWS is only used for already hospitalized patients. Furthermore, it does not use ECG information [48]. Additionally, it was not created for any specific disease but, rather, for an overall health assessment of an admitted patient in the ICU. Our objective is to use biomedical signal processing over easily acquirable signals to extract features to detect ST segments from ECG and to predict the symptoms of potential heart attack situations using the scoring system from warning signs from the biomedical signal analysis. Using the information from ECG, SPO2, and blood pressure, a new index system was proposed, and it was implemented in a MATLAB GUI.

The major symptoms of ECG wave related to MI are elevated ST segment, prolonged QT interval, pathological Q wave, hyperacute T wave, etc. [46,48]. Due to mobility and convenience, it is not possible to use all 12 leads for long-term monitoring. Additionally, muscle activity and other interference produce some abnormal trends from ECG which needs to be confirmed or supported. For this purpose, more biomedical signals need to be acquired and correlated with the ECG before making any final diagnosis decision. The most common reason behind heart failure is hypertension, which increases heart failure risk eightfold compared to fourfold [49,50]. For an accurate diagnosis, the markers for myocardial infarction from ECG should be supported by the level of hypertension or hypotension. Irregular heartbeat, which lowers the oxygenated blood, can be measured by observing a sudden drop in SpO2 levels. Research has shown that oxygen saturation lower than 93% is a sign of heart failure [51]. Also, a combination of specific systolic blood pressure and SpO2 lower than a certain threshold has definite diagnostic implications [52]. Since it was proven, in research, that the criteria of ST segment are the reason for higher sensitivity and specificity while diagnosing AMI, the maximum emphasis was given to ST segment detection [46].

In earlier studies, it was discovered that prolongation of the QT interval is correlated with MI or ventricular hypertrophy [53]. One of the several reasons behind the event of the abnormal T wave is when the T wave abnormality is consistent and occurs with an ST elevation [54]. Similarly, it was found in studies that a severe drop in blood pressure affects coronary perfusion and can cause deteriorating coronary events [54]. In this study, a fusion of the biomedical signals has been proposed where features from each sensor or source are considered to measure the abnormality, and then the fusion of the decision happens to provide the final verdict. Using the feature weights presented in Table 1, the local decision from ECG can be achieved. Based on all the local decisions, the final prediction will occur as a global decision. A detailed flowchart is given in Figure 8 where the steps were indicated to detect the ST segment from an ECG wave.

Table 1. The local threshold for ECG features.

ECG Threshold	ST Elevation	ST Depression	Hyperacute T Wave	Pathological Q Wave	Prolong Q Wave
single sensor	$\text{counter3}/\text{counter1} \geq 0.95$	$\text{mean_ST_dvalue} > 1$	$\text{abs}(\text{H_T_peak}) > 0.5$	$\text{mean_path_c} \leq -0.25$	$\text{mean_path_QT} > 0.4$
combination	$\text{counter3}/\text{counter1} \geq 0.95 \mid \text{mean_ST_dvalue} > 1$ then $e = 4$		$\text{mean_path_c} \leq -0.25 \mid \text{H_T_peak} > 0.5$ then $f = 1$		$\text{mean_path_QT} > 0.4$ then $g = 2$
need ECG monitoring consistency	$(e + f + g) > 0 \ \&\& \ (f + g) < 3 \ \&\& \ c_{ox} > 93 \ \&\& \ (c_{bp} \geq 105 \ \& \ c_{bp} \leq 120)$				
Potential MI scenario 1	$((e + f + g) > 0 \ \&\& \ (e + f + g) < 3) \ \&\& \ ((c_{bp} \geq 120 \ \mid \ c_{bp} < 105) \ \mid \ \mid \ \text{H_R} > 80 \ \mid \ c_{ox} < 93)$				
Potential MI scenario 2	$((e + f + g) > 0 \ \&\& \ (e + f + g) < 3) \ \&\& \ (c_{ox} > 93 \ \mid \ (c_{bp} \geq 105 \ \& \ c_{bp} \leq 120))$				
The initial case of MI	$(e + f + g) \geq 3 \ \&\& \ (((c_{bp} \geq 120 \ \& \ c_{bp} < 140) \ \mid \ (c_{bp} < 105 \ \& \ c_{bp} \geq 90)) \ \mid \ \mid \ \text{H_R} > 80 \ \mid \ (c_{ox} < 93 \ \& \ c_{ox} \geq 88))$				
Medium case of MI	$(e + f + g) \geq 3 \ \&\& \ ((c_{bp} \geq 120 \ \& \ c_{bp} < 140) \ \mid \ (c_{bp} < 105 \ \& \ c_{bp} \geq 90)) \ \mid \ \mid \ \text{H_R} > 80 \ \&\& \ (c_{ox} < 93 \ \& \ c_{ox} \geq 88)$				
A severe case of MI	$(e + f + g) > 3 \ \&\& \ (c_{bp} > 160 \ \mid \ c_{bp} < 90) \ \&\& \ c_{ox} < 88$				
Arrhythmia detected	$\text{H_R} > 80 \ \&\& \ (e + f + g) == 0$				
No MI symptoms	all normal				

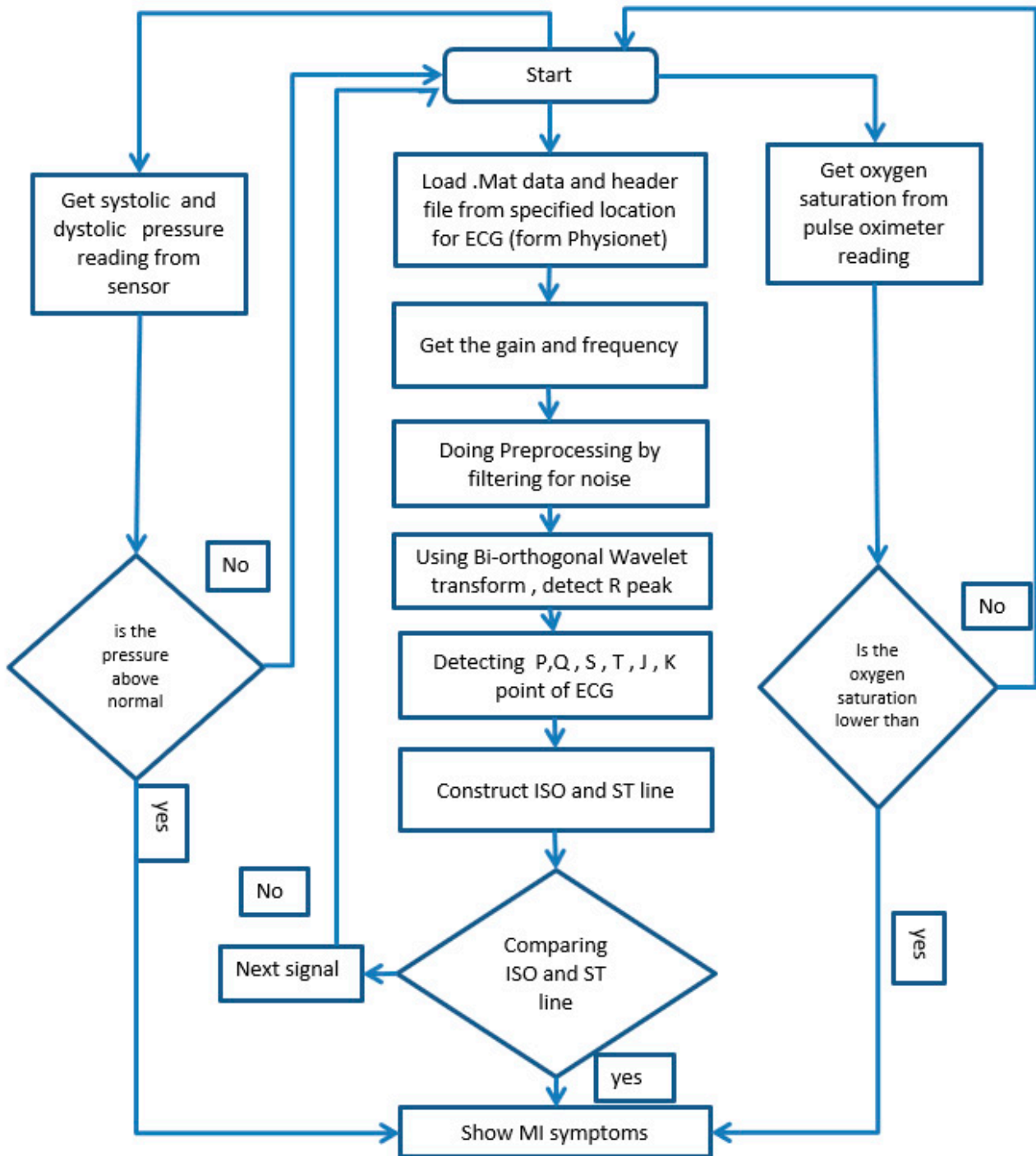


Figure 8. Flowchart for algorithm steps to get ST elevation in an ECG signal.

4. Biomedical Data Analysis

From the MIMIC dataset, patient’s data were collected as raw data. After necessary pre-processing to remove the interference and noise from those raw signals, the necessary features were extracted using the MATLAB GUI. The GUI is constructed in such a fashion that the input will be a raw signal, and the output will be extracted features, as well as some more features such as pulse transit time, which resulted in a calculation between ECG and PPG wave from the same patient. Two median filters were responsible to remove the baseband wander from the ECG wave, and a wavelet transform was used to remove the high-frequency noise. The iso-scale line was extracted so that the ST segment can be detected accurately. In Figure 9, an ECG signal with its baseline corrected has been shown.

Figure 10 depicted the use of wavelet transform, and Figure 11 shows the extracted peak from the ECG wave.

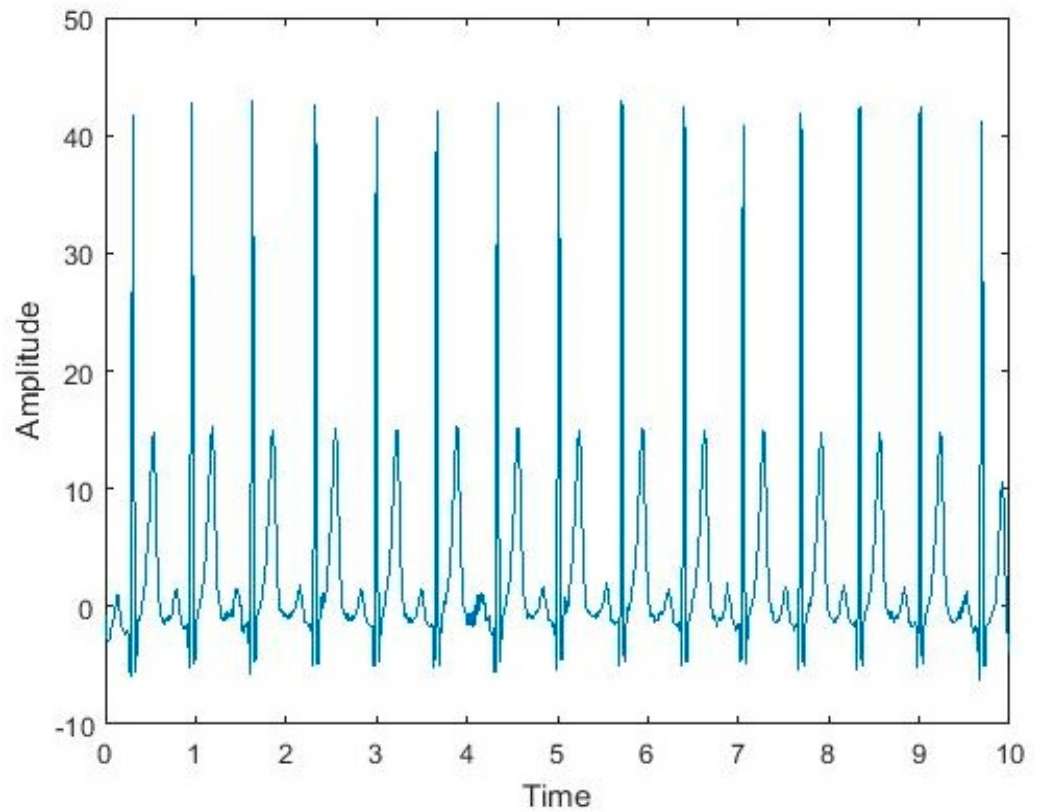


Figure 9. ECG signal with baseline wanders correction.

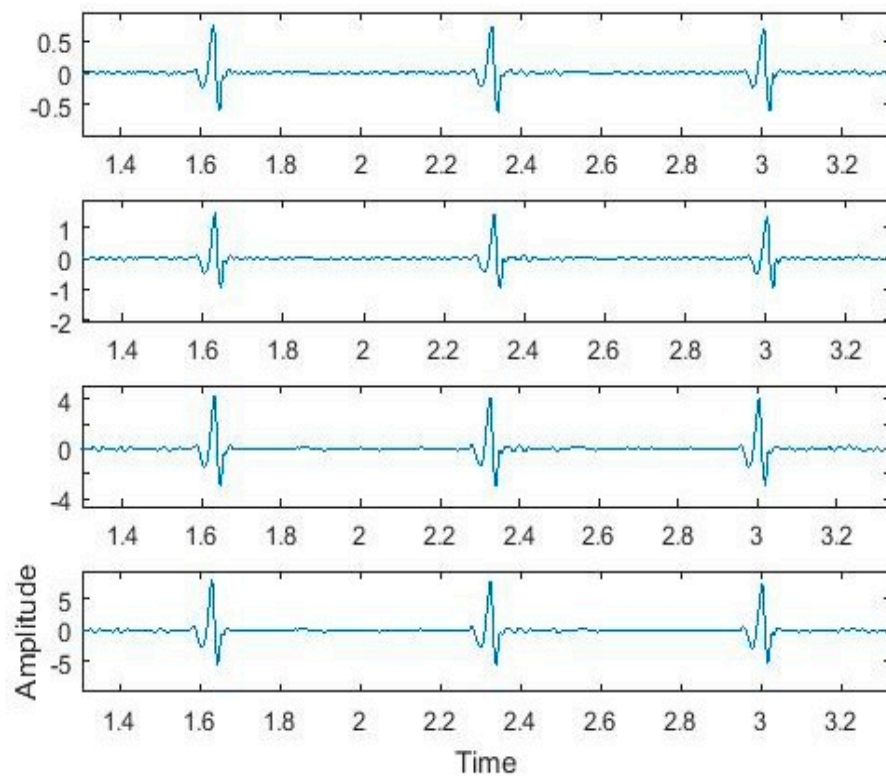


Figure 10. 2^1 to 2^4 level wavelet transform ECG signal.

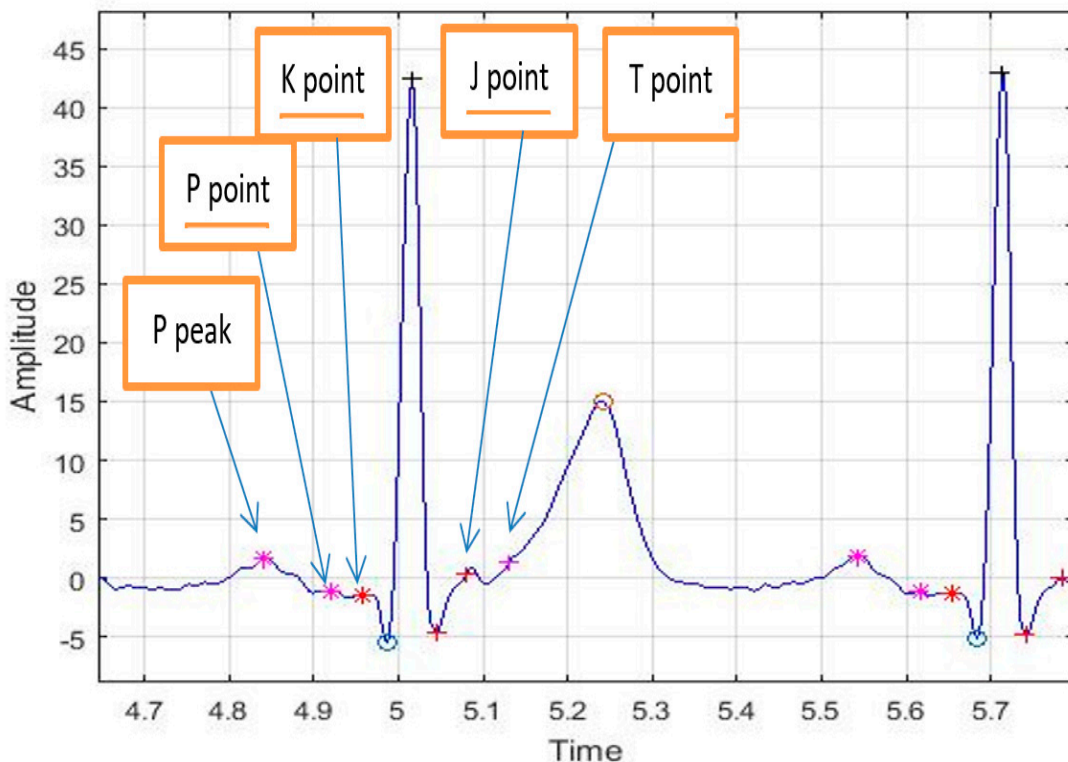


Figure 11. All peaks and points extracted (zoomed).

When an ECG waveform series come as an input, the GUI pre-processes, detects the peaks, and extracts the features if more than 95% ECG beat shows an elevated ST segment then ST elevation is concluded. There were some cases found when the ST elevation occurred for some ECG waves and did not stay up before or after. In some cases, the elevation is very abnormal and presented as a spike. Those cases were thrown out as misinterpretation. It is necessary to calculate, based on each ECG beat and after a certain window, to make a comparison overall to make sure the measurements are very consistent throughout the input signal. Figure 12 is shown where ST elevation was present.

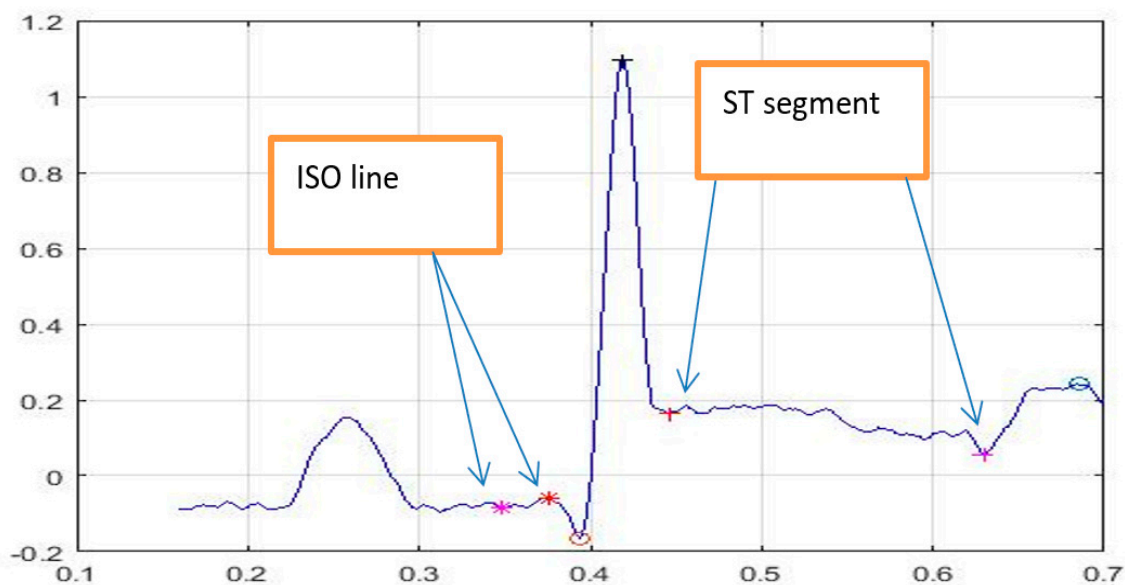


Figure 12. An example of ST elevation.

The three most significant symptoms of myocardial infarction (ST elevation, hyperacute T wave, and prolongation of the QT interval) maintain the characteristic of being present in contiguous leads. So, determining these features in a single lead may direct to a false output when the information from other leads is not accounted for. In Figure 13, examples are shown with information from leads I, II, and III to support the decision about MI. Here, it is evident that leads I, II, and III confirmed the existence of ST elevation in all of the beats, which qualifies as a symptom of myocardial infarction from an ECG signal. So, now, the next correlation with blood pressure and oximeter reading would make the detection more precise. Figures 14 and 15 show normal ECG with no ST elevation, or actual ST elevation, respectively.

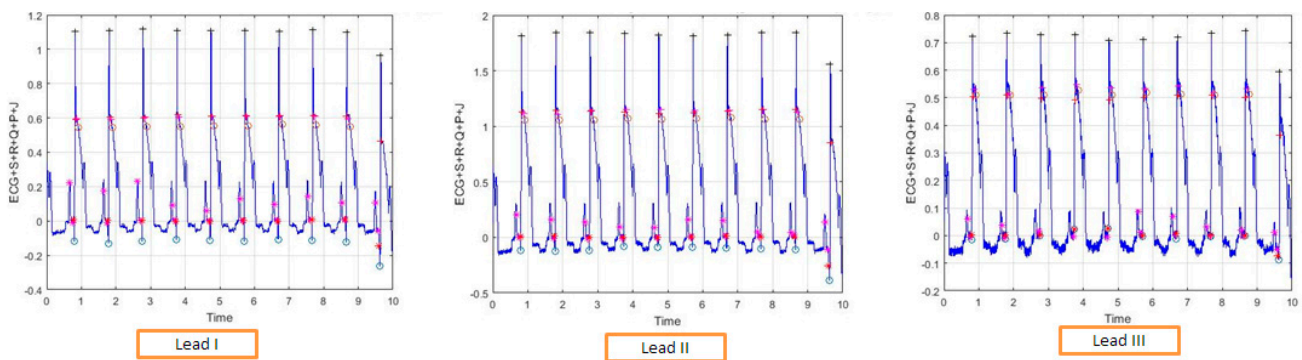


Figure 13. ST elevation in Lead I, II, and III.

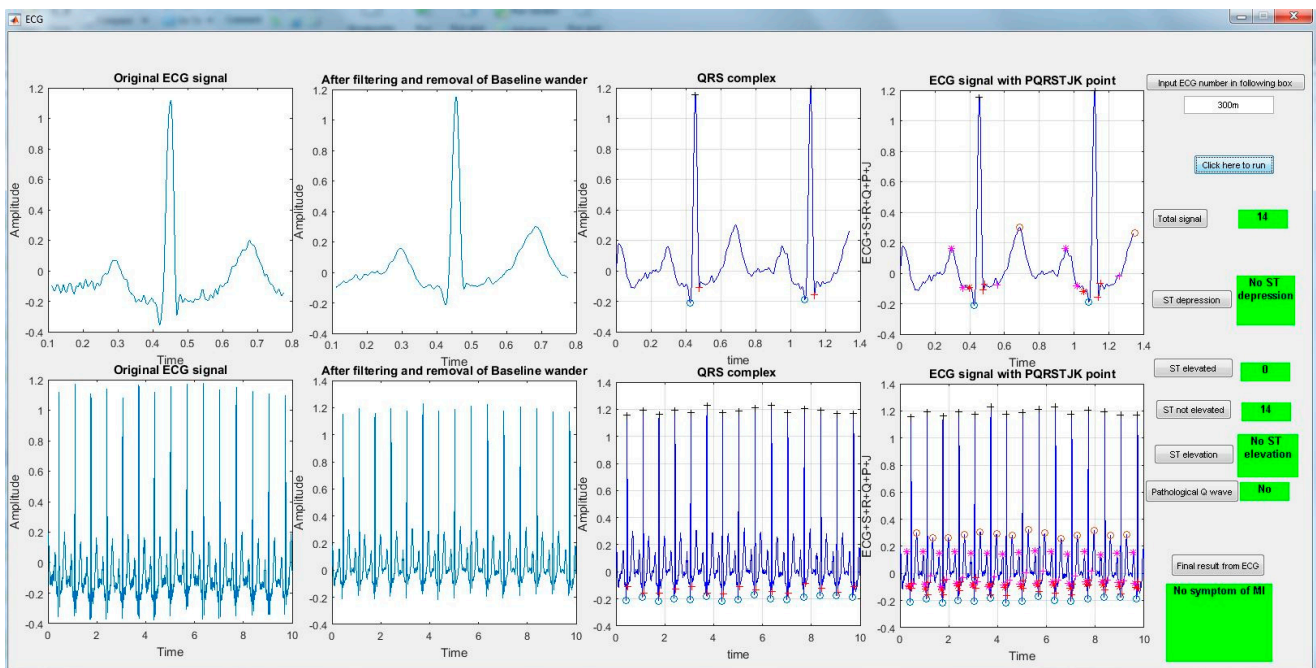


Figure 14. A normal ECG wave with no symptoms of MI.

The model also takes into account the measurement of blood pressure signals and oximeter readings. Those measurements were used in the algorithm to improve the reliability of the scoring system. By combining decisions from all three measurements (ECG, blood pressure, and oximeter), a conclusion can be drawn about the patient’s heart health. The diagram below contains four different ECG readings to differentiate the state of a heart condition. The extracted features, combining their impact on blood pressure and oxygen saturation to justify their respective heart condition, are ST elevation or depression, pathological Q wave, prolongation of QT interval, and inverted/hyper acute T wave. In Table 2, the threshold used

in the MATLAB program while creating the GUI has been depicted. Oxygen saturation tends to decrease concerning the increase of the deterioration of the myocardial infarction [49–55]. Additionally, the risk of myocardial infarction increases with the increase in systolic blood pressure [56]. Based on the sequential significance of the events related to oxygen saturation and blood pressure change, the thresholds were set in the table for fusion. Here, *c_bp* and *c_ox* are denoted as a measurement of systolic blood pressure and a measurement of oxygen saturation. Additionally, *e*, *f*, and *g* markers were used for the elevation of the ST segment, the hyperacute T wave, and the Q wave (prolonged).

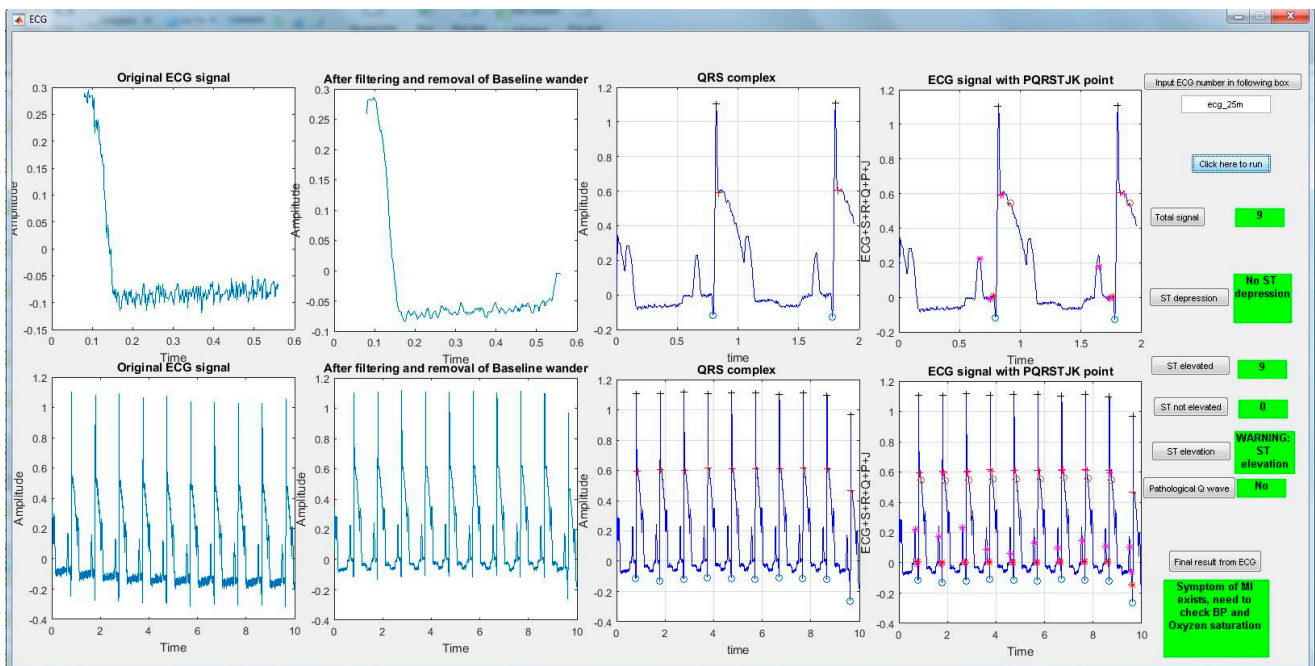


Figure 15. An ECG wave with the symptom of ST elevation.

Table 2. The threshold for decision fusion.

MI State	Decision Fusion
Needs ECG monitoring consistency	$(e + f + g) > 0 \ \&\& \ (f + g) < 3 \ \&\& \ c_{ox} > 93 \ \&\& \ (c_{bp} \geq 105 \ \&\& \ c_{bp} \leq 120)$
Potential MI scenario 1	$((e + f + g) > 0 \ \&\& \ (e + f + g) < 3) \ \&\& \ ((c_{bp} \geq 120 \ \ c_{bp} < 105) \ \ H_R > 80 \ c_{ox} < 93)$
Potential MI scenario 2	$((e + f + g) > 0 \ \&\& \ (e + f + g) < 3) \ \&\& \ (c_{ox} > 93 \ \ (c_{bp} \geq 105 \ \&\& \ c_{bp} \leq 120))$
The initial case of MI	$(e + f + g) \geq 3 \ \&\& \ (((c_{bp} \geq 120 \ \&\& \ c_{bp} < 140) \ \ (c_{bp} < 105 \ \&\& \ c_{bp} \geq 90)) \ \ H_R > 80 \ c_{ox} < 93 \ \&\& \ c_{ox} \geq 88)$
Medium case of MI	$(e + f + g) \geq 3 \ \&\& \ ((c_{bp} \geq 120 \ \&\& \ c_{bp} < 140) \ \ (c_{bp} < 105 \ \&\& \ c_{bp} \geq 90)) \ \ H_R > 80 \ \&\& \ (c_{ox} < 93 \ \&\& \ c_{ox} \geq 88)$
A severe case of MI	$(e + f + g) > 3 \ \&\& \ (c_{bp} > 160 \ \ c_{bp} < 90) \ \&\& \ c_{ox} < 88$
Arrhythmia detected	$H_R > 80 \ \&\& \ (e + f + g) == 0$
No MI symptoms	all normal

5. Performance Evaluation

The performance measures used here are the correlation coefficient, the F1 score, accuracy, false negative rate, false positive rate, false discover rate, precision, specificity, sensitivity, etc. The Physionet database was used for patient data [45]. Figure 16 has been depicted, where comparative performance measures were calculated using ECG and all three sensors.

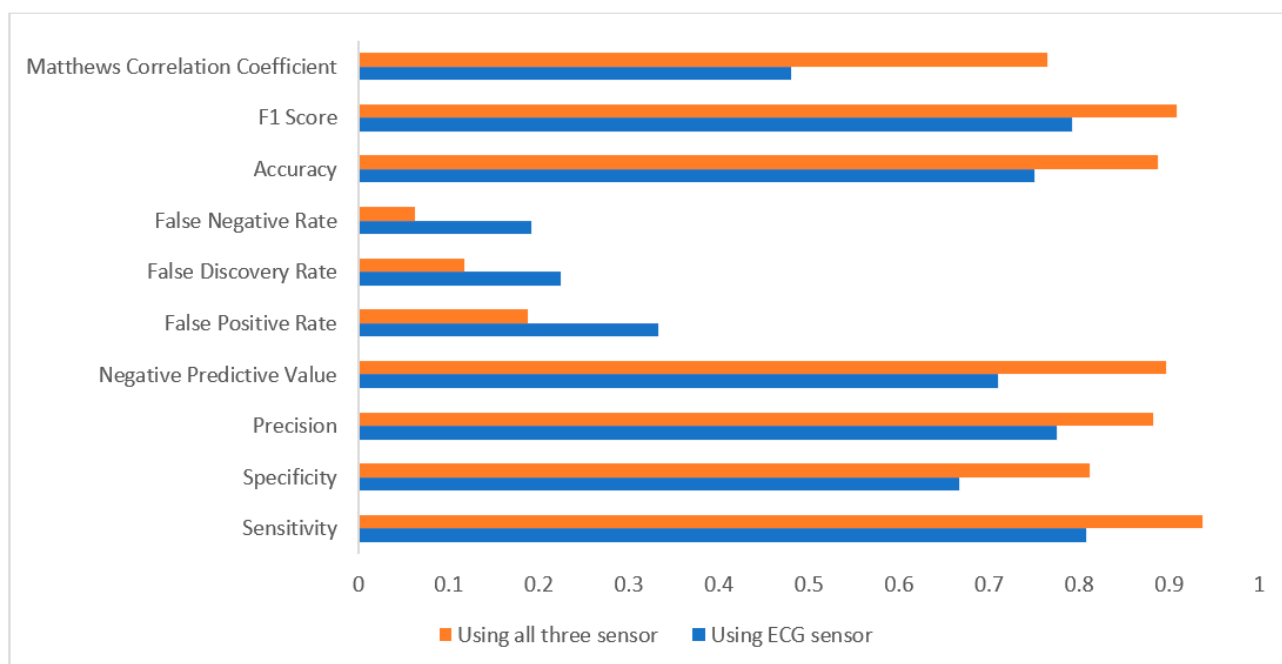


Figure 16. Assessment based on performance measures.

As shown in Figure 16, using information from ECG, the GUI output produces a false negative and false positive rate. Both of those reduced when all three sensors were used.

6. Discussion

Biomedical signal analysis of ECG signals, photoplethysmography (PPG) signals, pulse pressure signals, etc. are becoming very popular for diagnosing symptoms of complicated diseases. Until now, the most effective diagnosis of heart issues through biomedical signal analysis was arrhythmia detection using heartbeat count from an ECG signal, although this effective confines the research on count and only makes the scope of this kind of analysis very limited. The wealth of information available from ECG signals can be used, after analysis, to relate the change corresponding to symptoms of more complicated heart issues. At the same time, discoveries in biological science, such as the physical change of heart activity, changes in blood pressure, and oxygen saturation in blood, have to be taken into account for the reliable detection of symptoms. In this manuscript, the useful features from the ECG signal have been extracted to make sure that those features are consistent and relatable to myocardial infarction symptoms. Additionally, corresponding changes in blood pressure and oxygen saturation have been taken into account as well. The rationale behind the decision comes from the medical research, which dictates how a change in vital sign affected heart issues. In some studies, the researcher extracted features such as QRS and PT wavelength, PR, and RT interval. Although those features were useful, the dataset used was meant for arrhythmia [57]. When the bio-signals are used for patients with chronic heart conditions, the change in ECG from a normal wave is very prominent. At the same time, analyzing abnormal ECG and detecting these features precisely are much more difficult. The proposed MATLAB GUI is responsible for detecting the features from the ECG signal of a heart patient, which is an improvement over detecting those symptoms of a normal patient. There has been much research in recent times where machine learning or deep learning techniques were used to relate the raw ECG signal with different heart conditions [58–62]. All those studies classify ECG signals into different heart health or disease, but there are two main drawbacks. First, these techniques require a large amount of training data and are computationally very extensive. Second, these techniques cannot explain how the models work. Researchers need to work on a robust model with improvement in ability to explain the success of the model. Because of these

reasons, despite a large number of studies, there is a very small number compared to those which ended up in practical implementation.

There were several limitations involved in the studies presented in this paper. First, the number of patients could have been higher to achieve a better distribution of characteristics in patients. Second, the focus was on the the ST segment, the hyperacute T wave, the prolonged QT interval, etc., based on medical research. More investigation needs to be conducted to find more reliable features from ECG with MI to improve the accuracy. Third, the variation of change in different features of ECG, due to different stages of a particular heart condition, is not limited to a certain range. In some cases, the change in ECG comes close to a scenario that can easily be assumed as an abnormal (incorrect) ECG measurement. The MATLAB GUI needs to be more robust to be able to detect such unusual ECG behavior accurately. Simple implementation and techniques will allow that to be used or incorporated in a user-friendly way. More studies and experiments are required for the larger dataset to make this model robust.

7. Conclusions and Future Work

This paper uses the biomedical signal analysis of ECG, oximeter reading, and blood pressure to extract useful features for fusion for a more accurate prediction of MI and the detection of ST segment. A MATLAB GUI was developed, which uses the biomedical signals (raw) as inputs and produces the ST detection and diagnosis of MI. The process starts with the input of raw signals, pre-processing such as noise and interference removal, detection of peaks, and measurement of features. Using data from the online dataset of the physio next, the model was evaluated.

For rhythm-related heart conditions, only ECG can provide us sufficient information, but several other significant heart diseases such as sinus bradycardia, sinus tachycardia, atrial flutter, ventricular flutter, etc., and significant symptoms hidden in the ECG signal of an individual, can strengthen the conformity of the disease, and the patient can take precautionary actions to avoid severe consequence in future. To make sure the detection is false alarm free, the input from other sensors such as blood pressure and oximeter readings need to be considered and correlated with the ECG signal. For remote health monitoring, the automation will help an individual to have a quick and accurate idea about their current heart condition. The future objective is to implement the fusion of sensors to bring one final result within an automated system. The implementation will be an extension of the fusion model proposed in this paper, along with a suitable decision technique.

Funding: This research received no external funding.

Institutional Review Board Statement: Not applicable.

Informed Consent Statement: Not applicable.

Data Availability Statement: <https://archive.physionet.org/physiobank/database/mimicdb/> (accessed on 10 July 2022).

Conflicts of Interest: The author declares no conflict of interest.

References

1. De Chazal, P.; O'Dwyer, M.; Reilly, R.B. Automatic classification of heartbeats using ECG morphology and heartbeat interval features. *IEEE Trans. Biomed. Eng.* **2004**, *51*, 1196–1206. [[CrossRef](#)] [[PubMed](#)]
2. Palaniappan, R.; Krishnan, S.M. Detection of ectopic heart beats using ECG and blood pressure signals. In Proceedings of the 2004 International Conference on Signal Processing and Communications, SPCOM'04, Beijing, China, 31 August–4 September 2004; pp. 573–576.
3. Lovell, N.H.; Magrabi, F.; Celler, B.G.; Huynh, K.; Garsden, H. Web-Based acquisition, storage, and retrieval of biomedical signals. *IEEE Eng. Med. Biol. Mag.* **2001**, *20*, 38–44. [[CrossRef](#)] [[PubMed](#)]
4. Xia, H.; Asif, I.; Zhao, X. Cloud-ECG for real time ECG monitoring and analysis. *Comput. Methods Programs Biomed.* **2013**, *110*, 253–259. [[CrossRef](#)] [[PubMed](#)]

5. Mamun, K.; Rahman, M.M.; Alouani, A. Automatic detection of heart diseases using biomedical signals: A literature review of current status and limitations. In Proceedings of the Future of Information and Communication Conference, San Francisco, CA, USA, 3–4 March 2022; pp. 420–440.
6. Wiharto, W.; Kusnanto, H.; Herianto, H. Intelligence system for diagnosis level of coronary heart disease with K-star algorithm. *Healthc. Inform. Res.* **2016**, *22*, 30–38. [[CrossRef](#)]
7. Bashir, S.; Qamar, U.; Khan, F.H. A multicriteria weighted vote-based classifier ensemble for heart disease prediction. *Comput. Intell.* **2016**, *32*, 615–645. [[CrossRef](#)]
8. Daraei, A.; Hamidi, H. An Efficient Predictive Model for Myocardial Infarction Using Cost-sensitive J48 Model. *Iran. J. Public. Health* **2017**, *46*, 682–692.
9. Dutta, A.; Batabyal, T.; Basu, M. An efficient convolutional neural network for coronary heart disease prediction. *Expert Syst. Appl.* **2020**, *159*, 113408. [[CrossRef](#)]
10. Li, Y.; He, Z.; Wang, H. CraftNet: A deep learning ensemble to diagnose cardiovascular diseases. *Biomed. Signal Process. Control* **2020**, *62*, 102091. [[CrossRef](#)]
11. Ahsan, M.M.; Nazim, R.; Siddique, Z.; Huebner, P. Detection of COVID-19 patients from CT scan and chest X-ray data using modified MobileNetV2 and LIME. *Healthcare* **2021**, *9*, 1099. [[CrossRef](#)]
12. Ahsan, M.M.; Ahad, M.T.; Soma, F.A. Detecting SARS-CoV-2 from chest X-Ray using artificial intelligence. *IEEE Access* **2021**, *9*, 35501–35513. [[CrossRef](#)]
13. Verma, S.; Gupta, A. Effective prediction of heart disease using data mining and machine learning: A review. In Proceedings of the 2021 International Conference on Artificial Intelligence and Smart Systems (ICAIS), Coimbatore, India, 25–27 March 2021; pp. 249–253.
14. Hoodbhoy, Z.; Jiwani, U.; Sattar, S.; Salam, R.; Hasan, B.; Das, J.K. Diagnostic accuracy of machine learning models to identify congenital heart disease: A meta-analysis. *Front. Artif. Intell.* **2021**, *4*, 97. [[CrossRef](#)] [[PubMed](#)]
15. Rath, A.; Mishra, D.; Panda, G.; Satapathy, S.C. An exhaustive review of machine and deep learning based diagnosis of heart diseases. *Multimed. Tools Appl.* **2021**, *81*, 36069–36127. [[CrossRef](#)]
16. Benhar, H.; Idri, A.; Fernández-Alemán, J. Data preprocessing for heart disease classification: A systematic literature review. *Comput. Methods Programs Biomed.* **2020**, *195*, 105635. [[CrossRef](#)] [[PubMed](#)]
17. Thakor, N.V.; Zhu, Y. Applications of adaptive filtering to ECG analysis: Noise cancellation and arrhythmia detection. *IEEE Trans. Biomed. Eng.* **1991**, *38*, 785–794. [[CrossRef](#)]
18. Axelsson, M.; Dang, Q.; Pitsillides, K.; Munns, S.; Hicks, J.; Kassab, G.S. A novel, fully implantable, multichannel biotelemetry system for measurement of blood flow, pressure, ECG, and temperature. *J. Appl. Physiol.* **2007**, *102*, 1220–1228. [[CrossRef](#)] [[PubMed](#)]
19. Zhou, S.H.; Rautaharju, P.M.; Calhoun, H.P. Selection of a reduced set of parameters for classification of ventricular conduction defects by cluster analysis. In Proceedings of the Computers in Cardiology Conference, London, UK, 5–8 September 1993; pp. 879–882.
20. Herrero, G.G.; Gotchev, A.; Christov, I.; Egiazarian, K. Feature extraction for heartbeat classification using independent component analysis and matching pursuits. In Proceedings of the (ICASSP'05) IEEE International Conference on Acoustics, Speech, and Signal Processing, Philadelphia, PA, USA, 23 March 2005; Volume 4, pp. iv/725–iv/728.
21. Gay, V.; Leijdekkers, P. A Health Monitoring System Using Smart Phones and Wearable Sensors. *Int. J. Assist. Robot. Mechatron.* **2007**, *8*, 29–36.
22. Baloglu, U.B.; Talo, M.; Yildirim, O.; San Tan, R.; Acharya, U.R. Classification of myocardial infarction with multi-lead ECG signals and deep CNN. *Pattern Recog. Lett.* **2019**, *122*, 23–30. [[CrossRef](#)]
23. Wasimuddin, M.; Elleithy, K.; Abuzneid, A.; Faezipour, M.; Abuzaghleh, O. Multiclass ECG signal analysis using global average-based 2-D convolutional neural network modeling. *Electronics* **2021**, *10*, 170. [[CrossRef](#)]
24. Tang, X.; Hu, Q.; Tang, W. A real-time QRS detection system with PR/RT interval and ST segment measurements for wearable ECG sensors using parallel delta modulators. *IEEE Trans. Biomed. Circuits Syst.* **2018**, *12*, 751–761. [[CrossRef](#)]
25. Campero Jurado, I.; Fedjajevs, A.; Vanschoren, J.; Brombacher, A. Interpretable Assessment of ST-Segment Deviation in ECG Time Series. *Sensors* **2022**, *22*, 4919. [[CrossRef](#)]
26. Jurado, I.C.; Vanschoren, J. Multi-Fidelity optimization method with asynchronous generalized island model for AutoML. In Proceedings of the Genetic and Evolutionary Computation Conference Companion, Boston, MA, USA, 9–13 July 2022; pp. 220–223.
27. Tao, R.; Zhang, S.; Huang, X. Magnetocardiography-Based ischemic heart disease detection and localization using machine learning methods. *IEEE Trans. Biomed. Eng.* **2018**, *66*, 1658–1667. [[CrossRef](#)] [[PubMed](#)]
28. Han, C.; Shi, L. Automated interpretable detection of myocardial infarction fusing energy entropy and morphological features. *Comput. Methods Programs Biomed.* **2019**, *175*, 9–23. [[CrossRef](#)] [[PubMed](#)]
29. Zhang, G.; Si, Y.; Wang, D.; Yang, W.; Sun, Y. Automated detection of myocardial infarction using a gramian angular field and principal component analysis network. *IEEE Access* **2019**, *7*, 171570–171583. [[CrossRef](#)]
30. AlZu'bi, S.; Shehab, M.; Al-Ayyoub, M.; Jararweh, Y.; Gupta, B. Parallel implementation for 3d medical volume fuzzy segmentation. *Pattern Recog. Lett.* **2020**, *130*, 312–318. [[CrossRef](#)]

31. Zhang, X.; Li, R.; Dai, H.; Liu, Y.; Zhou, B.; Wang, Z. Localization of myocardial infarction with multi-lead bidirectional gated recurrent unit neural network. *IEEE Access* **2019**, *7*, 161152–161166. [[CrossRef](#)]
32. Zhang, J.; Lin, F.; Xiong, P. Automated detection and localization of myocardial infarction with staked sparse autoencoder and treebagger. *IEEE Access* **2019**, *7*, 70634–70642. [[CrossRef](#)]
33. Wang, H.; Li, Z.; Li, Y.; Gupta, B.B.; Choi, C. Visual saliency guided complex image retrieval. *Pattern Recog. Lett.* **2020**, *130*, 64–72. [[CrossRef](#)]
34. Hammad, M.; Alkinani, M.H.; Gupta, B.; El-Latif, A.; Ahmed, A. Myocardial infarction detection based on deep neural network on imbalanced data. *Multimed. Syst.* **2022**, *28*, 1373–1385. [[CrossRef](#)]
35. Northern Sami. SVG Human Heart Cross-Section. Available online: [https://commons.wikimedia.org/wiki/File:Diagram_of_the_human_heart_\(cropped\).svg](https://commons.wikimedia.org/wiki/File:Diagram_of_the_human_heart_(cropped).svg) (accessed on 8 August 2022).
36. Peterson, E.D.; Shah, B.R.; Parsons, L. Trends in quality of care for patients with acute myocardial infarction in the National Registry of Myocardial Infarction from 1990 to 2006. *Am. Heart J.* **2008**, *156*, 1045–1055. [[CrossRef](#)]
37. Hasdai, D.; Behar, S.; Wallentin, L. A prospective survey of the characteristics, treatments and outcomes of patients with acute coronary syndromes in Europe and the Mediterranean basin. The Euro Heart Survey of Acute Coronary Syndromes (Euro Heart Survey ACS). *Eur. Heart J.* **2002**, *23*, 1190–1201. [[CrossRef](#)]
38. Thygesen, K.; Alpert, J.S.; White, H.D. Universal definition of myocardial infarction. *J. Am. Coll. Cardiol.* **2007**, *50*, 2173–2195. [[CrossRef](#)] [[PubMed](#)]
39. Fernández, J.C. New Methodologies for the Development and Validation of Electrophysiological Models. Ph.D. Thesis, Universidad de Zaragoza, Zaragoza, Spain, 2019.
40. Whitmer, K.H. Assessment of Pulmonary Function. In *A Mixed Course-Based Research Approach to Human Physiology*; Iowa State University Digital Press: Ames, IA, USA, 2021.
41. Chobanian, A.V.; Bakris, G.L.; Black, H.R. The seventh report of the joint national committee on prevention, detection, evaluation, and treatment of high blood pressure: The JNC 7 report. *JAMA* **2003**, *289*, 2560–2571. [[CrossRef](#)] [[PubMed](#)]
42. Myocardial Infarction. Available online: https://commons.wikimedia.org/wiki/File:Myocardial_infarction.svg (accessed on 8 August 2022).
43. Atanasova, G.; Marinov, M. The pulse pressure amplitude as a marker of myocardial infarction risk. *J. Clin. Exp. Cardiol.* **2013**, *4*, 2. [[CrossRef](#)]
44. Mamun, M.M.R.K.; Alouani, A.T. Myocardial infarction detection using multi biomedical sensors. In Proceedings of the 10th International Conference on Bioinformatics and Computational Biology, Las Vegas, NV, USA, 19–21 March 2018; pp. 117–122.
45. PhysioBank. PhysioNet. Available online: <https://archive.physionet.org> (accessed on 19 April 2017).
46. Martin, T.N.; Groenning, B.A.; Murray, H.M. ST-Segment deviation analysis of the admission 12-lead electrocardiogram as an aid to early diagnosis of acute myocardial infarction with a cardiac magnetic resonance imaging gold standard. *J. Am. Coll. Cardiol.* **2007**, *50*, 1021–1028. [[CrossRef](#)]
47. Jouck, P. *Application of the Wavelet Transform Modulus Maxima Method to T-Wave Detection in Cardiac Signals*; Maastricht University, Department of Mathematics and Maastricht Instruments: Maastricht, The Netherlands, 2004; pp. 1–32.
48. Masip, J.; Gayà, M.; Páez, J.; Betbesé, A.; Vecilla, F.; Manresa, R.; Ruiz, P. Pulse oximetry in the diagnosis of acute heart failure. *Rev. Española Cardiol.* **2012**, *65*, 879–884. [[CrossRef](#)]
49. Kannel, W.B.; Levy, D.; Cupples, L.A. Left ventricular hypertrophy and risk of cardiac failure: Insights from the Framingham Study. *J. Cardiovasc. Pharmacol.* **1987**, *10* (Suppl. 6), S135–S140. [[CrossRef](#)] [[PubMed](#)]
50. Lip, G. Hypertensive heart disease: A complex syndrome or a hypertensive cardiomyopathy? *Eur. Heart J.* **2000**, *21*, 1653–1665. [[CrossRef](#)]
51. Ramirez-Carracedo, R.; Sanmartin, M.; Ten, A.; Hernandez, I.; Tesoro, L.; Diez-Mata, J.; Botana, L.; Ovejero-Paredes, K.; Filice, M.; Alberich-Bayarri, A.; et al. Theranostic contribution of extracellular matrix metalloprotease inducer-paramagnetic nanoparticles against acute myocardial infarction in a pig model of coronary ischemia-reperfusion. *Circ. Cardiovasc. Imaging* **2022**, *15*, e013379. [[CrossRef](#)]
52. Milo-Cotter, O.; Cotter, G.; Kaluski, E. Rapid clinical assessment of patients with acute heart failure: First blood pressure and oxygen saturation—Is that all we need? *Cardiology* **2009**, *114*, 75–82. [[CrossRef](#)]
53. Wong, N.D.; Levy, D.; Kannel, W.B. Prognostic significance of the electrocardiogram after Q wave myocardial infarction. The Framingham Study. *Circulation* **1990**, *81*, 780–789. [[CrossRef](#)]
54. Channer, K.; Morris, F. ABC of clinical electrocardiography: Myocardial ischaemia. *BMJ* **2002**, *324*, 1023–1026. [[CrossRef](#)] [[PubMed](#)]
55. Candil, J.J.; Luengo, C.M. QT interval and acute myocardial ischemia: Past promises, new evidences. *Rev. Esp. Cardiol.* **2008**, *61*, 561–563.
56. Psaty, B.M.; Furberg, C.D.; Kuller, L.H. Association between blood pressure level and the risk of myocardial infarction, stroke, and total mortality: The cardiovascular health study. *Arch. Intern. Med.* **2001**, *161*, 1183–1192. [[CrossRef](#)] [[PubMed](#)]
57. Taloba, A.I.; Alanazi, R.; Shahin, O.R.; Elhadad, A.; Abozeid, A.; El-Aziz, A.; Rasha, M. Machine algorithm for heartbeat monitoring and arrhythmia detection based on ECG systems. *Comput. Intell. Neurosci.* **2021**, *2021*, 7677568. [[CrossRef](#)]

58. Hakraborty, A.; Chatterjee, S.; Majumder, K.; Shaw, R.N.; Ghosh, A. A comparative study of myocardial infarction detection from ECG data using machine learning. In *Advanced Computing and Intelligent Technologies*; Springer: Cham, Switzerland, 2022; pp. 257–267.
59. Wang, J. Advances in ECG-Based Cardiac Ischemia Monitoring—A Review. In Proceedings of the 2021 Computing in Cardiology (CinC), Brno, Czech Republic, 12–15 September 2021; Volume 48, pp. 1–4.
60. Wang, H.; Zhao, W.; Xu, Y. ST segment change classification based on multiple feature extraction using ECG. In Proceedings of the 2018 Computing in Cardiology Conference (CinC), Maastricht, The Netherlands, 23–26 September 2018; pp. 1–4.
61. Bigler, M.R.; Seiler, C. Detection of myocardial ischemia by intracoronary ECG using convolutional neural networks. *PLoS ONE* **2021**, *16*, e0253200. [[CrossRef](#)]
62. Zhao, Y.; Xiong, J.; Hou, Y. Early detection of ST-segment elevated myocardial infarction by artificial intelligence with 12-lead electrocardiogram. *Int. J. Cardiol.* **2020**, *317*, 223–230. [[CrossRef](#)]